



# From the ground up: microhabitat use within a landscape context frames the spatiotemporal scale of settlement and vacancy dynamics in an endemic habitat specialist

Danielle K. Walkup · Wade A. Ryberg · Lee A. Fitzgerald · Toby J. Hibbitts

Received: 14 November 2018 / Accepted: 15 September 2019  
© Springer Nature B.V. 2019

## Abstract

**Context** Understanding how species are distributed throughout landscapes requires knowledge of the hierarchy of habitat selection made by individuals, the resulting spatiotemporal structure of demography, and the consequent dynamics of localized populations.

**Objectives** We examined how patterns of habitat use, settlement, and vacancy in an endemic habitat specialist, *Sceloporus arenicolus* (dunes sagebrush lizard), varied within the Mescalero Monahans Sandhills ecosystem.

**Methods** We used a 4-year mark-recapture dataset to develop occupancy models that identified whether microhabitat or landscape scale best predicted *S. arenicolus* spatiotemporal habitat use, settlement, and vacancy, in both an undisturbed and disturbed landscape.

**Results** Our results showed areas of high quality habitat were used constantly and lower quality areas were used intermittently, but repeatedly, over time in the undisturbed landscape. Habitat use in the disturbed landscape was spatiotemporally unpredictable. Microhabitat variables characterizing dune landscape topography predicted probability of use in *S. arenicolus*, while landscape-scale variables predicted probabilities of settlement and vacancy. In the undisturbed landscape, future settlement was predicted by presence of *S. arenicolus*, a pattern consistent with fine-scale source-sink dynamics already described for this species.

**Conclusions** Our results illustrate how spatially-discrete but temporally-linked areas should be conserved at fine spatiotemporal scales to secure

**Electronic supplementary material** The online version of this article (<https://doi.org/10.1007/s10980-019-00909-5>) contains supplementary material, which is available to authorized users.

D. K. Walkup (✉)

Natural Resources Institute, Department of Wildlife and Fisheries Sciences, Texas A&M University, 2260 TAMU, 578 John Kimbrough Blvd., College Station, TX 77843, USA  
e-mail: dkwalkup@tamu.edu

W. A. Ryberg

Natural Resources Institute, Texas A&M University, 2260 TAMU, 578 John Kimbrough Blvd., College Station, TX 77843, USA

L. A. Fitzgerald

Biodiversity, Research and Teaching Collection, Department of Wildlife and Fisheries Sciences, Texas A&M University, 2258 TAMU, Wildlife, Fisheries, and Ecological Science Building, College Station, TX 77843, USA

T. J. Hibbitts

Biodiversity, Research and Teaching Collection, Natural Resources Institute, Department of Wildlife and Fisheries Sciences, Texas A&M University, 2258 TAMU, Wildlife, Fisheries and Ecological Science Building, College Station, TX 77843, USA

persistence of *S. arenicolus* populations under variable environmental conditions. Disturbances to habitat continuity can disrupt individual movements and create inconsistently occupied habitat patches that appear to be unoccupied and thus are threatened by further disturbances.

**Keywords** Mescalero Monahans Sandhill ecosystem · Fragmentation · Habitat use · *Sceloporus arenicolus* · Ecological scaling · Habitat specialist

## Introduction

Understanding how the spatiotemporal distribution of individuals within landscapes affects population dynamics and species' persistence is an overarching question in ecology (Turner and Chapin 2005). Even continuous habitats are not usually homogenous but can be made up of a mosaic of resource patches (Merriam 1995; Shaver 2005; Webb et al. 2017). The configuration of these mosaics of varying quality influences species' distributions through patterns of dispersal of individuals, populations, and species across landscapes over time (González-Megías et al. 2005; Turner and Chapin 2005; Ryberg and Fitzgerald 2016). Knowing how a species is distributed across the landscape is especially important in conservation contexts, as variation in habitat quality can drive population persistence in patchy landscapes (Ye et al. 2013a, b; Webb et al. 2017).

Knowing how species are distributed throughout their habitat requires understanding the hierarchical use of habitat of the species (Levin 1992; Wiens et al. 1993). Because the movements of individuals scale up to broader patterns of occupancy and distribution, characterizing distribution patterns at smaller scales can be helpful in determining the scalar nature of habitat use and inform conservation aims (Wiens et al. 1993). Both microhabitat and larger landscape patterns influence the dynamics of how individuals move and settle among different quality habitats (Frey et al. 2012; Herse et al. 2017). While landscape characteristics are perhaps more easily understood and more often considered, microhabitat characteristics add important information and improve predictions of population parameters such as density, abundance, and occupancy (Cornell and Donovan 2010; McClure et al.

2012; Webb et al. 2017). For example, Michael et al. (2017) showed that both microhabitat and landscape scale variables were important for predicting occupancy of many reptile species in a woodland-agriculture matrix. Many important population processes (e.g., survival, recruitment) are local in scale, but vary over time and space (Krohne and Burgin 1990).

Habitat specialists in particular frequently exhibit patterns of occupancy that are spatiotemporally variable, where dynamics are governed by a hierarchical scaling of habitat use (e.g. Bicknell's thrush (*Catharus bicknelli*), Frey et al. 2012; Eurasian reed warbler (*Acrocephalus scirpaceus*), Sozio et al. 2013). *Sceloporus arenicolus* (dunes sagebrush lizard), for example, is an endemic habitat specialist regionally restricted to the Mescalero-Monahans Sandhills ecosystem of West Texas and southeast New Mexico (Fitzgerald and Painter 2009; Laurencio and Fitzgerald 2010). Within this ecosystem, *S. arenicolus* exclusively uses the mosaic of dune blowouts in a shinnery oak matrix (Fitzgerald et al. 1997; Fitzgerald and Painter 2009). Dune blowouts range continuously in size from a few meters wide to tens of meters wide. At the microhabitat scale, individual *S. arenicolus* typically prefer, but are not restricted to, larger blowouts characterized by steeper slopes, lower substrate compaction, medium sand grain sizes, and less vegetative cover (Smolensky and Fitzgerald 2011; Ryberg et al. 2012; Hibbitts et al. 2013; Ryberg and Fitzgerald 2015). At a larger scale, *S. arenicolus* are patchily distributed in neighborhoods (sensu Addicott et al. 1987, localized groups of interacting individuals within a continuously distributed population; Ryberg et al. 2013), and survivorship and fecundity in neighborhoods is tightly linked to habitat configuration (Ryberg et al. 2015). In particular, the pattern of dune blowouts across the landscape appears to create source and sink neighborhoods (Ryberg et al. 2013) such that even in continuous areas of habitat considered highly likely to contain *S. arenicolus*, we do not always find them (Walkup et al. 2018). Thus, while the spatial hierarchy of habitat use in this system is well understood, the temporal micro-variation in neighborhood occupancy within this hierarchy is not.

To gain insight into this spatiotemporal, micro-variation in neighborhood occupancy, we develop models that characterize determinants of habitat use, settlement, and vacancy (i.e., occupancy, colonization, and extinction sensu lato) at both the microhabitat and

larger landscape scales (Betts et al. 2008; Efford and Dawson 2012; McClure and Hill 2012). By including in our models both microhabitat and landscape variables that reflect habitat features selected within and across *S. arenicolus* home ranges, respectively (Hibbitts et al. 2013; Ryberg et al. 2013; Young et al. 2018), we seek to determine which scale better predicts *S. arenicolus* spatiotemporal habitat use and therefore distribution. More importantly, by incorporating dynamics of settlement and vacancy along with use, we aim to determine the scale and identity of habitat features that predict whether an area or neighborhood is constantly occupied, intermittently used, or not used at all.

From a conservation perspective, identifying intermittently used areas (i.e. areas used in some years but not others) is critical to the persistence of this species, because habitats deemed unoccupied, even after very few surveys, can be mistakenly viewed as never occupied. Such habitats are routinely developed for oil and gas extraction and, more recently, sand mining industries leading to regional habitat fragmentation, population isolation, reduced population sizes, stochastic demography, and eventual local extirpations (Smolensky and Fitzgerald 2011; Leavitt and Fitzgerald 2013; Walkup et al. 2017). Given the growing prevalence of these habitat threats in the region (e.g., Texas accounted for ~ 44% of total US crude oil output in November 2016; U.S. Energy Information Administration (EIA) 2017; Pierre et al. 2018; Wolaver et al. 2018a, b), we also develop models to characterize determinants of habitat use, settlement, and vacancy at both microhabitat and larger landscape scales for a population occupying an area undergoing oil and gas development. By focusing on populations in disturbed as well as undisturbed areas, we attempt to determine how and at what scale variation in occupancy might vary spatiotemporally in the future as this entire ecosystem changes rapidly.

## Methods

### Study sites

The Mescalero-Monahans Sandhills ecosystem (MMS) of West Texas and southeast New Mexico is a self-organized, semi-stabilized dune system formed and maintained by wind patterns eroding and depositing sand against stabilizing shinnery oak (*Quercus*

havardii; Fitzgerald and Painter 2009; Laurencio and Fitzgerald 2010). Regionally, the MMS persists in a landscape mosaic of mesquite (*Prosopis glandulosa*) flats and shinnery oak flats. Oil and natural gas extraction has been occurring within the MMS since the early 1900s and has followed a boom-bust pattern of expansion and inactivity based on economic drivers (Galley 1958; Haggerty et al. 2014). In periods of expansion, well-pads and roads are constructed at very fast rates, with the number of permitted wells more than doubling in the Permian basin between 2008 and 2012 (Wolaver et al. 2018b). Well-pads and roads in the MMS are created by bulldozing areas and covering them with a layer of caliche (a calcium carbonate-based soil, excavated from surrounding areas), which maintains a hard-packed road surface. These roads and well-pads are the primary source of habitat loss and fragmentation in the MMS. Our study site was located on the edge of oil and gas expansion in Andrews County, Texas.

### Trapping

Two 13.69 ha (370 m × 370 m) trapping arrays large enough to encompass hundreds of overlapping *S. arenicolus* home ranges in addition to several oil and gas well pads and roads were installed in May 2012. Each of the two trapping arrays consisted of 36 sub-grids (3 × 3 arrays with 10 m spacing) spaced 50 m apart to make a 6 × 6 array of sub-grids (Online Appendix Fig. 5). The 50 m spacing was twice the average daily movement length for *S. arenicolus* (Young et al. 2018), which made the sub-grids effectively independent within trapping sessions but not across trapping sessions, an ideal design for characterizing variation in settlement and vacancy. Traps were 20-l buckets buried with rims flush to the ground, with 40 cm × 40 cm plywood cover boards propped 1–2 inches high (Fitzgerald 2012). One array was constructed in disturbed habitat with 3 oil well-pads in and around it and a road cutting through it. The other array was in relatively undisturbed habitat. On the disturbed array, three sub-grids in the southeast corner were eliminated because a well-pad was installed in that area over the winter of 2012. Sampling occurred from April through August 2012–2015. Each trapping session lasted 7 days in 2012 and 5 days in 2013–2015. There were five trap sessions during May–August 2012. With the change to 5-day trapping

periods, there were nine trap sessions each year during April–August 2013–2015. Traps were checked and cleared every 24 h.

#### Microhabitat variables

Microhabitat variables were measured at each trap in 2014: slope (degrees); substrate compaction (Lang penetrometer); and percent cover for six cover types (sand, shinnery oak, yucca/shrubs, forbs/grasses, caliche, and litter). The microhabitat data were averaged for each sub-grid and a Principal Components Analysis (PCA) with the covariance matrix was used to reduce dimensionality and identify the main sources of variation for microhabitat in each sub-grid. The data were transformed using log transformations (slope and penetrometer) or arc-sine transformations (percent cover variables) to better meet normality assumptions of the test (Gotelli and Ellison 2004). The first two PCA axis scores were then used as independent variables in subsequent analyses.

#### Landscape variables

A supervised classification of 1-m resolution color infrared (false-color) National Agriculture Imagery Program (NAIP) imagery in 4-bands (red, green, blue, and near infrared) from 2014 (Retrieved in January 2015; <http://gis.apfo.usda.gov/arcgis/services/>) was used to determine five cover classes (sand, shinnery oak, mesquite, grass, and caliche) across *S. arenicolus*' range in Texas, creating a raster for each class. A 35 m buffer was used to clip these rasters around each array. Because sand and caliche classes are hard to distinguish based on spectral reflectance values, these two cover classes were merged and considered sand. To get the caliche cover class, polygons were hand drawn covering roads and well-pads and merged into the raster, leaving us with five cover classes: sand, shinnery oak, mesquite, grass, and road/well-pad. Rasters were divided into a 6 × 6 grid encompassing 70 m × 70 m, creating 36 landscapes, each centered on one trapping sub-grid (Fig. 5).

Fragstats v. 4.2 (McGarigal et al. 2012) was used to estimate class metrics for each landscape: mean patch size (ha) for sand, shinnery oak, and the road/well-pad cover layers; total edge for sand, shinnery oak, and the road/well-pad cover layers; fractal dimension for sand and shinnery oak cover layers, and clumpiness index

for sand and shinnery oak cover layers. Fractal dimension represents the mean shape complexity of patches in each cover class on a scale of 1, where the mean focal patch is an Euclidean shape (like a square or circle) to 2, where the mean focal patch has a highly convoluted perimeter (Turner 1990). The clumpiness index measures the mean degree of aggregation of patches in each cover class across the landscape on a scale of – 1, where the focal patch is maximally disaggregated, to 1, where the focal class is maximally aggregated. These class metrics were chosen because previous research has shown that metrics of these types have predictive value for *S. arenicolus* population parameters (Ryberg et al. 2013, 2015). Total edge was removed after constructing a correlation matrix because it was highly correlated with other variables (e.g. mean patch size, fractal dimension, and clumpiness). The final retained variables had Pearson's *r* from – 0.43 to 0.57 for the undisturbed array and – 0.61 to 0.52 for the disturbed array. Finally, a Principal Components Analysis (PCA), using program PAST v 3.19 (Hammer et al. 2001), was performed on the landscape datasets from each array to identify the main sources of variation in the datasets and reduce dimensionality. We retained the top two principal component axes (PC) from each analysis.

#### Modeling

Following the approach developed by MacKenzie et al. (2003), dynamic occupancy models were used to estimate patterns of settlement and vacancy in the microhabitat and local landscape of the sampling arrays. Because patterns of how microhabitat influences distribution of individuals across landscapes in two continuous populations were being measured, model parameters are best expressed as use, settlement, and vacancy (following Betts et al. 2008; Efford and Dawson 2012; McClure and Hill 2012), instead of occupancy, colonization, and local extinction, respectively. Here, use is the probability that *S. arenicolus* will be present in a given sub-grid, settlement is the probability that a sub-grid that was un-used in the previous time period would be used in the current time period, and vacancy is the probability that a sub-grid that was used in the previous time period had no *S. arenicolus* detected in the current time period. In this case, settlement and vacancy represent apparent movement, because we are not following marked

individuals. Additionally, the density of individuals at a site can influence settlement and vacancy estimates depending on the locations of individuals and their territories. Trap data were aggregated into a presence-absence matrix for each sub-grid. To satisfy the assumption of closure within a season, each trap session was considered a “season” and the trap-days were the repeat surveys. Then, each sample year (2012–2015) was analyzed separately because of the 6-month interval without trapping between each activity season. This resulted in 16 sets of models, 4 years for each of the following: undisturbed array—microhabitat scale, undisturbed array—landscape scale, disturbed array—microhabitat scale, and disturbed array—landscape scale.

Multiple models were developed to understand relationships of both microhabitat and landscape variables using package `unmarked` (Fiske and Chandler 2011) in R v. 3.4.2 (R Core Team 2018). For each sub-grid individually, use, settlement, vacancy, and detection were modeled as functions of the PC axis scores using microhabitat variables in one set of models and landscape variables in a separate set of models. The top two PC axes scores for each of the array—scale combinations above were included (named: UM1, UM2, UL1, UL2, DM1, DM2, DL1, and DL2). Each axis is interpreted in the results and described in Online Appendix Table 5. Each trapping occasion was included as a time covariate for settlement, vacancy, and detection. Finally, an autocovariate was included to account for the influence of spatial autocorrelation of *S. arenicolus* detections in our models. This was modeled as  $AUTO_i = \sum W_{ij} Y_j / \sum W_{ij}$  where  $W_{ij}$  = the inverse geographic distance between sub-grids *i* and *j* and  $Y_j$  = the presence of *S. arenicolus* in sub-grid *j* (i.e. 1 if present, 0 if absent) (Augustin et al. 1996; Betts et al. 2006; Chammem et al. 2012). This autocovariate returns an index from 0 (none of the surrounding sub-grids are occupied) to 1 (all of the surrounding sub-grids are occupied) for each sub-grid in each trapping occasion. Neither the time covariate nor the spatial autocorrelation covariate were included for the use parameter, which is the use at the initial time period ( $\psi_i$ ).

Because of limited data, each parameter was modeled as a function of each covariate singly or as an additive relationship between all possible combinations of two covariates. Detection (*p*) was modeled

first, holding the other parameters constant. Any covariates in the top detection models ( $\Delta AICc < 2$ ) were retained and used to model use ( $\psi$ ), holding settlement ( $\gamma$ ) and vacancy ( $\epsilon$ ) constant. Those steps were repeated to model vacancy, then settlement to get the final set of models run. Finally, for each set of models, to estimate the betas, SE, and 95% CI's for each parameter, the models were model averaged (using the models containing the given covariate) in `AICcmodavg` (Mazerolle 2016), following the procedure in Buckland et al. (1997) and Burnham and Anderson (2002). Abbreviated AICc model results are presented in Table 1, the full model results are in Tables 5–8 in the Online Appendix. The beta and 95% CI's for the variables from the model averaged results are presented in Figs. 1 and 2 and Tables 9–12 in the Online Appendix. Inference was drawn from covariates with the most weight in the top models from Tables 1 and 5–8 in the Online Appendix. Values reported in the text are model averaged parameter estimates plus or minus one standard error. Figures 6–13 in the Online Appendix shows the relationships of the variables to the parameters. For brevity, variables related to detection probability are fully described in the appendix to allow greater focus on use, settlement, and vacancy parameters.

## Results

### Trapping

Over the 4 years of trapping (2012–2015), the two arrays were operational for 125,712 trap-days (2012, *n* = 26,568; 2013, *n* = 33,048; 2014, *n* = 35,640; 2015, *n* = 30,456). During this time, we captured 12,814 lizards of 8 species, of which 1539 were *S. arenicolus*. Of the total captures of *S. arenicolus*, 726 individuals were captured: 549 on the undisturbed array and 177 on the disturbed array. Of 813 total recaptures, 681 were on the undisturbed array and 132 on the disturbed array.

### Principal components analysis

The first two PC axes explained 57.2 and 18.4% of the variation in microhabitat on the undisturbed array, and 50.6 and 24.5% of the variation on the disturbed array (Online Appendix Table 3). These

**Table 1** Top 3 models or models with  $\Delta AIC \leq 2$  for each set of models

|                          | Year                  | Model       |                   |                        | nPars                | AIC        | $\Delta AIC$ | AICwt  | cumltvWt |      |      |
|--------------------------|-----------------------|-------------|-------------------|------------------------|----------------------|------------|--------------|--------|----------|------|------|
| Undisturbed-microhabitat | 1                     | $\psi(UM1)$ | $\gamma(.)$       | $\varepsilon(UM2 + A)$ | $p(UM1 + S)$         | 11         | 627.97       | 0.00   | 0.30     | 0.30 |      |
|                          |                       | $\psi(UM1)$ | $\gamma(.)$       | $\varepsilon(UM2 + A)$ | $p(UM1 + S)$         | 12         | 629.48       | 1.51   | 0.14     | 0.44 |      |
|                          | 2                     | $\psi(UM2)$ | $\gamma(S)$       | $\varepsilon(UM2+S)$   | $p(UM1)$             | 21         | 1051.53      | 0.00   | 0.16     | 0.16 |      |
|                          |                       | $\psi(UM2)$ | $\gamma(A+S)$     | $\varepsilon(UM2+S)$   | $p(UM1)$             | 22         | 1051.80      | 0.26   | 0.14     | 0.29 |      |
|                          |                       | $\psi(UM2)$ | $\gamma(UM1 + S)$ | $\varepsilon(UM2+S)$   | $p(UM1)$             | 22         | 1052.23      | 0.70   | 0.11     | 0.40 |      |
|                          | 3                     | $\psi(UM2)$ | $\gamma(UM1)$     | $\varepsilon(UM1)$     | $p(UM1 + S)$         | 16         | 894.29       | 0.00   | 0.36     | 0.36 |      |
|                          |                       | $\psi(UM2)$ | $\gamma(UM1+A)$   | $\varepsilon(UM1)$     | $p(UM1 + S)$         | 17         | 896.27       | 1.99   | 0.13     | 0.49 |      |
|                          |                       | $\psi(UM2)$ | $\gamma(UM1)$     | $\varepsilon(UM1+A)$   | $p(UM1 + S)$         | 17         | 896.29       | 2.00   | 0.13     | 0.62 |      |
|                          | 4                     | $\psi(UM1)$ | $\gamma(A)$       | $\varepsilon(UM1)$     | $p(UM1)$             | 8          | 860.66       | 0.00   | 0.10     | 0.10 |      |
|                          |                       | $\psi(UM1)$ | $\gamma(.)$       | $\varepsilon(UM1)$     | $p(UM1)$             | 7          | 860.85       | 0.19   | 0.10     | 0.20 |      |
|                          |                       | $\psi(UM1)$ | $\gamma(.)$       | $\varepsilon(UM1 + A)$ | $p(UM1)$             | 8          | 861.12       | 0.46   | 0.08     | 0.28 |      |
|                          | Undisturbed-landscape | 1           | $\psi(.)$         | $\gamma(A + S)$        | $\varepsilon(UL1)$   | $p(A + S)$ | 14           | 681.79 | 0.00     | 0.11 | 0.11 |
| $\psi(UL2)$              |                       |             | $\gamma(A + S)$   | $\varepsilon(UL1)$     | $p(A + S)$           | 15         | 682.44       | 0.66   | 0.08     | 0.18 |      |
| $\psi(UL1)$              |                       |             | $\gamma(A + S)$   | $\varepsilon(UL1)$     | $p(A + S)$           | 15         | 682.93       | 1.14   | 0.06     | 0.24 |      |
| 2                        |                       | $\psi(.)$   | $\gamma(UL1 + A)$ | $\varepsilon(UL2)$     | $p(UL1 + S)$         | 16         | 1117.40      | 0.00   | 0.20     | 0.20 |      |
|                          |                       | $\psi(UL2)$ | $\gamma(UL1 + A)$ | $\varepsilon(UL2)$     | $p(UL1 + S)$         | 17         | 1118.68      | 1.29   | 0.10     | 0.30 |      |
|                          |                       | $\psi(.)$   | $\gamma(A+S)$     | $\varepsilon(UL2)$     | $p(UL1 + S)$         | 22         | 1119.20      | 1.80   | 0.08     | 0.38 |      |
| 3                        |                       | $\psi(UL1)$ | $\gamma(A)$       | $\varepsilon(UL2 + A)$ | $p(UL2 + S)$         | 17         | 974.67       | 0.00   | 0.13     | 0.13 |      |
|                          |                       | $\psi(.)$   | $\gamma(A)$       | $\varepsilon(UL2 + A)$ | $p(UL2 + S)$         | 16         | 974.88       | 0.21   | 0.12     | 0.24 |      |
|                          |                       | $\psi(UL1)$ | $\gamma(UL2 + A)$ | $\varepsilon(UL2 + A)$ | $p(UL2 + S)$         | 18         | 975.45       | 0.79   | 0.09     | 0.33 |      |
| 4                        |                       | $\psi(UL2)$ | $\gamma(A)$       | $\varepsilon(.)$       | $p(UL1)$             | 7          | 902.51       | 0.00   | 0.04     | 0.04 |      |
|                          |                       | $\psi(UL2)$ | $\gamma(UL1+A)$   | $\varepsilon(.)$       | $p(UL1)$             | 8          | 902.89       | 0.38   | 0.03     | 0.07 |      |
|                          |                       | $\psi(UL2)$ | $\gamma(A)$       | $\varepsilon(UL2)$     | $p(UL1)$             | 8          | 903.02       | 0.51   | 0.03     | 0.11 |      |
| Disturbed-microhabitat   |                       | 1           | $\psi(DM2)$       | $\gamma(.)$            | $\varepsilon(DM2+S)$ | $p(.)$     | 9            | 257.99 | 0.00     | 0.06 | 0.06 |
|                          |                       |             | $\psi(DM2)$       | $\gamma(DM1)$          | $\varepsilon(DM2+S)$ | $p(.)$     | 10           | 258.23 | 0.24     | 0.05 | 0.12 |
|                          | $\psi(DM2)$           |             | $\gamma(.)$       | $\varepsilon(DM2+S)$   | $p(A)$               | 10         | 259.12       | 1.13   | 0.03     | 0.15 |      |
|                          | 2                     | $\psi(DM1)$ | $\gamma(DM2+S)$   | $\varepsilon(DM1)$     | $p(DM1+A)$           | 17         | 384.23       | 0.00   | 0.27     | 0.27 |      |
|                          |                       | $\psi(DM1)$ | $\gamma(DM2+S)$   | $\varepsilon(DM1+A)$   | $p(DM1+A)$           | 16         | 384.60       | 0.37   | 0.22     | 0.49 |      |
|                          |                       | $\psi(.)$   | $\gamma(DM2)$     | $\varepsilon(A+S)$     | $p(DM1)$             | 14         | 406.69       | 0.00   | 0.13     | 0.13 |      |
|                          | 3                     | $\psi(DM2)$ | $\gamma(DM2)$     | $\varepsilon(A+S)$     | $p(DM1)$             | 15         | 407.45       | 0.76   | 0.09     | 0.21 |      |
|                          |                       | $\psi(.)$   | $\gamma(DM2+A)$   | $\varepsilon(A+S)$     | $p(DM1)$             | 15         | 407.55       | 0.86   | 0.08     | 0.30 |      |
|                          |                       | $\psi(DM2)$ | $\gamma(DM1+S)$   | $\varepsilon(DM2+A)$   | $p(DM2)$             | 16         | 590.60       | 0.00   | 0.73     | 0.73 |      |
|                          | Disturbed-landscape   | 1           | $\psi(.)$         | $\gamma(A+S)$          | $\varepsilon(UL1)$   | $p(A+S)$   | 14           | 681.79 | 0.00     | 0.11 | 0.11 |
|                          |                       |             | $\psi(UL2)$       | $\gamma(A+S)$          | $\varepsilon(UL1)$   | $p(A+S)$   | 15           | 682.44 | 0.66     | 0.08 | 0.18 |
|                          |                       |             | $\psi(UL1)$       | $\gamma(A+S)$          | $\varepsilon(UL1)$   | $p(A+S)$   | 15           | 682.93 | 1.14     | 0.06 | 0.24 |
| 2                        |                       | $\psi(.)$   | $\gamma(UL1 + A)$ | $\varepsilon(UL2)$     | $p(UL1+S)$           | 16         | 1117.40      | 0.00   | 0.20     | 0.20 |      |
|                          |                       | $\psi(UL2)$ | $\gamma(UL1 + A)$ | $\varepsilon(UL2)$     | $p(UL1+S)$           | 17         | 1118.68      | 1.29   | 0.10     | 0.30 |      |
|                          |                       | $\psi(.)$   | $\gamma(A + S)$   | $\varepsilon(UL2)$     | $p(UL1+S)$           | 22         | 1119.20      | 1.80   | 0.08     | 0.38 |      |
| 3                        |                       | $\psi(UL1)$ | $\gamma(A)$       | $\varepsilon(UL2 + A)$ | $p(UL2 + S)$         | 17         | 974.67       | 0.00   | 0.13     | 0.13 |      |
|                          |                       | $\psi(.)$   | $\gamma(A)$       | $\varepsilon(UL2 + A)$ | $p(UL2 + S)$         | 16         | 974.88       | 0.21   | 0.12     | 0.24 |      |
|                          |                       | $\psi(UL1)$ | $\gamma(UL2 + A)$ | $\varepsilon(UL2 + A)$ | $p(UL2 + S)$         | 18         | 975.45       | 0.79   | 0.09     | 0.33 |      |
| 4                        |                       | $\psi(UL2)$ | $\gamma(A)$       | $\varepsilon(.)$       | $p(UL1)$             | 7          | 902.51       | 0.00   | 0.04     | 0.04 |      |
|                          |                       | $\psi(UL2)$ | $\gamma(UL1 + A)$ | $\varepsilon(.)$       | $p(UL1)$             | 8          | 902.89       | 0.38   | 0.03     | 0.07 |      |
|                          |                       | $\psi(UL2)$ | $\gamma(A)$       | $\varepsilon(UL2)$     | $p(UL1)$             | 8          | 903.02       | 0.51   | 0.03     | 0.11 |      |

Shared model covariates: (.) = constant model; A = autocovariate; S = Session (time effect). Undisturbed Landscape model covariates: UL1 = large, aggregated sand patches to small, disaggregated sand patches gradient; UL2 = large, complex shinnery oak patches to small, simple shinnery oak patches gradient. Disturbed Landscape model covariates: DL1 = large shinnery oak patches to large sand and road-wellpad patches gradient; DL2 = highly aggregated sand patches to complex sand and shinnery oak patches gradient. Undisturbed Microhabitat model covariates: UM1 = high average slope to high average compaction gradient; UM2 = high to low percent cover of oak and litter gradient. Disturbed Microhabitat model covariates: DM1 = high average slope to high average compaction gradient; DM2 = high oak and litter cover to high sand cover gradient. For full  $\Delta AIC \leq 2$  model set, see Online Appendix Tables 5–8

axis scores were used as independent covariates in settlement and vacancy models. On both undisturbed and disturbed arrays, the first PC axis (UM1 and DM1, respectively) represented a slope and compaction gradient, where higher average slopes corresponded with lower average compaction values. Larger dunes with steeper slopes tend to have looser sand, which makes for a less compact substrate, while flatter areas correspond with more compact soils that support mesquite grassland or areas covered with caliche. On the undisturbed array, the second PC axis (UM2) captured a gradient of high to low percent shinnery oak and percent litter cover. On the disturbed array, the second PC axis (DM2) also captured variation in cover types, with percent sand cover on one end of the gradient and percent shinnery oak and percent litter cover on the other. Since shinnery oak is the densest vegetation on our arrays, this likely represented a cover gradient from dense vegetation to more open sandy areas.

The first two PC axes explained 29.3 and 26.2% of the variance in landscape configuration on the undisturbed array, and 35.0 and 21.7% on the disturbed array, and were retained as covariates in the models (Online Appendix Table 3). On the undisturbed array, the first PC axis (UL1) represented a gradient from large, aggregated sand patches to small, more dispersed sand patches. The second PC axis (UL2) captured a gradient of large areas of shinnery oak corresponding with high fractal dimensions for shinnery oak patches, indicating a gradient from larger, complex shinnery oak patches to smaller, simpler shinnery oak patches. On the disturbed array, the first PC axis (DL1) represented a gradient where large areas of sand and patches of caliche for roads and well-pads contrasted with large patches of shinnery oak, indicating that sand and road/well-pad patches dominated in some areas, while shinnery oak patches dominated others. The second PC axis (DL2) captured a gradient of larger fractal dimensions of sand and oak patches contrasted with high clumpiness values for sand patches, indicating that more highly aggregated sand patches had less complex patch shape, and that complex shapes of sand patches correlated with complex shapes of shinnery oak patches.

## Models

### Use

On the undisturbed array, there was a repeated pattern of use during this study (Tables 1, 2). In year 1, the probability of use of sub-grids by *S. arenicolus* was restricted to areas with larger, more extensive blow-outs on the west side of the array where mean slope increased and mean substrate compaction decreased (UM1; Fig. 3; Fig. 8a in Online Appendix). There was a low probability of use on the east side of the array, where blowouts were smaller and the landscape transitioned to flatter mesquite grasslands (Fig. 3; Fig. 8b in Online Appendix). In years 2 and 3, probability of use increased as the percent cover of shinnery oak (UM2) increased. This corresponded with a spread in the population to the east side of the undisturbed array (Fig. 3; Fig. 8b in Online Appendix), along with higher capture rates for *S. arenicolus* (Online Appendix Table 4). Finally, in year 4, the population was mostly using the largest dune areas on the west side of the array again, characterized by high mean slope and low mean substrate compaction (Fig. 3, Fig. 8a in Online Appendix).

In the disturbed array, we also quantified a dynamic response by *S. arenicolus* to the microhabitat features, but no repeating patterns of use were observed (Tables 1, 2). Instead, there were two small, disjunct areas of very high use in the north and southwestern parts of the array that shifted spatially in years 1, 2, and 4 (Fig. 3). In year 3, probability of use was very low over the whole array ( $\psi = 0.07 \pm 0.06$ ; Fig. 3). In years 1 and 4, probability of use increased as percent cover of sand increased and percent covers of shinnery oak and litter decreased (DM2; Fig. 3; Fig. 8c in Online Appendix). Probability of use for year 2 increased as mean slope increased and mean compaction decreased (DM1; Fig. 3; Fig. 8d in Online Appendix).

For landscape models at both arrays, model results for the probability of use for all years showed that landscape variables measured generally did not have a higher AICc than the constant use model (Table 1). On the undisturbed array, probability of use increased slowly each year in years 1 through 3 then declined slightly in year 4 (Fig. 3; Fig. 9a in Online Appendix). On the undisturbed array, year 3 had an increase in probability of use as area and clumpiness of sand

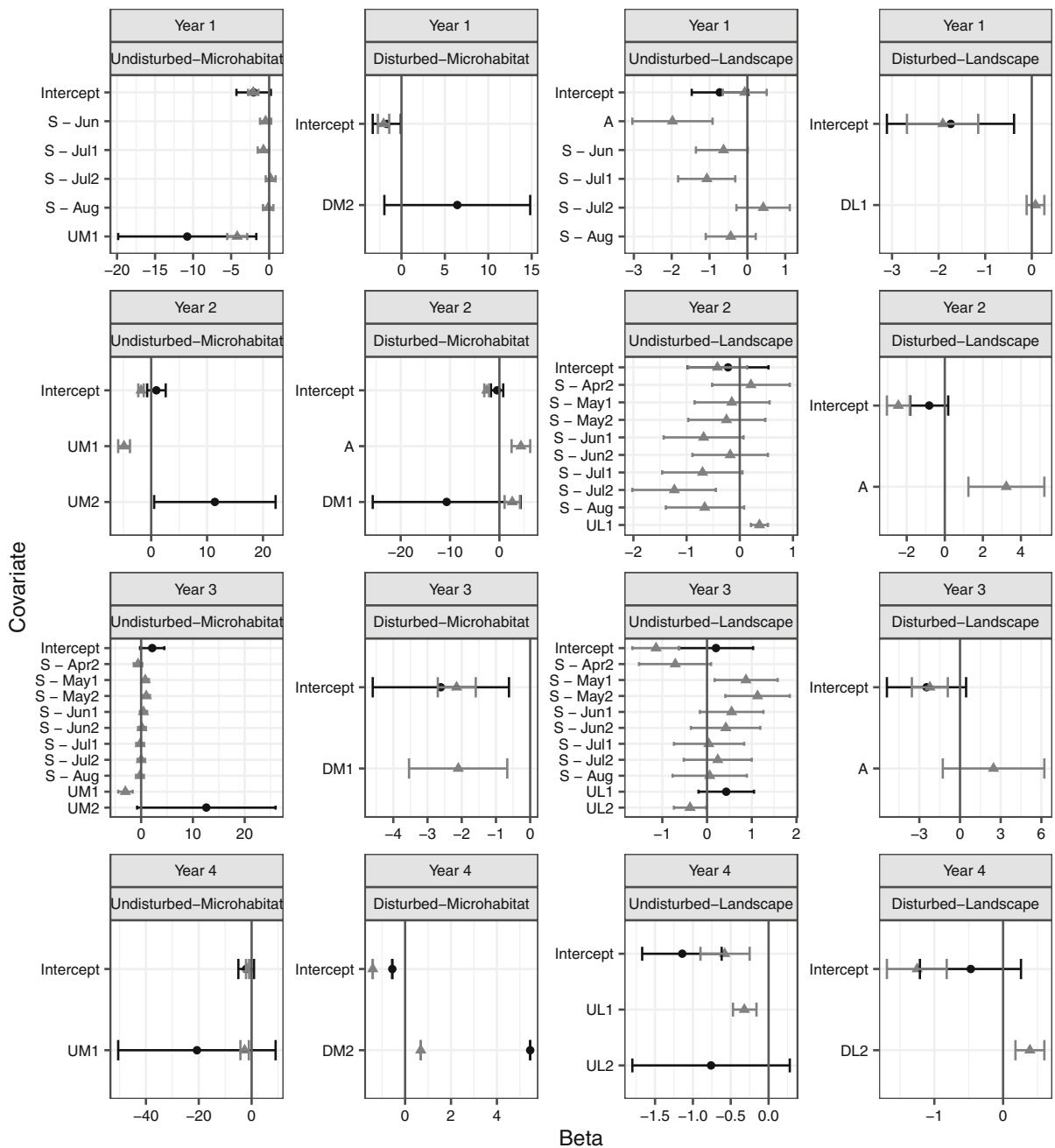


**Fig. 1** Model averaged beta values and 95% Confidence Intervals for probability of use ( $\psi$ ; black circles) and detection ( $p$ ; gray triangles)

increased (UL1); in year 4, probability of use decreased as area and fractal dimension of oak patches increased (UL2; Fig. 3). On the disturbed array, years 2 and 4 had slightly higher probabilities of use than years 1 and 3 (Fig. 3; Fig. 9b in Online Appendix).

*Settlement and vacancy*

For microhabitat models, probability of settlement at both arrays had no consistent predictor variables (Tables 1, 2; Fig. 10 in Online Appendix). In the undisturbed array, in year 1, probability of settlement



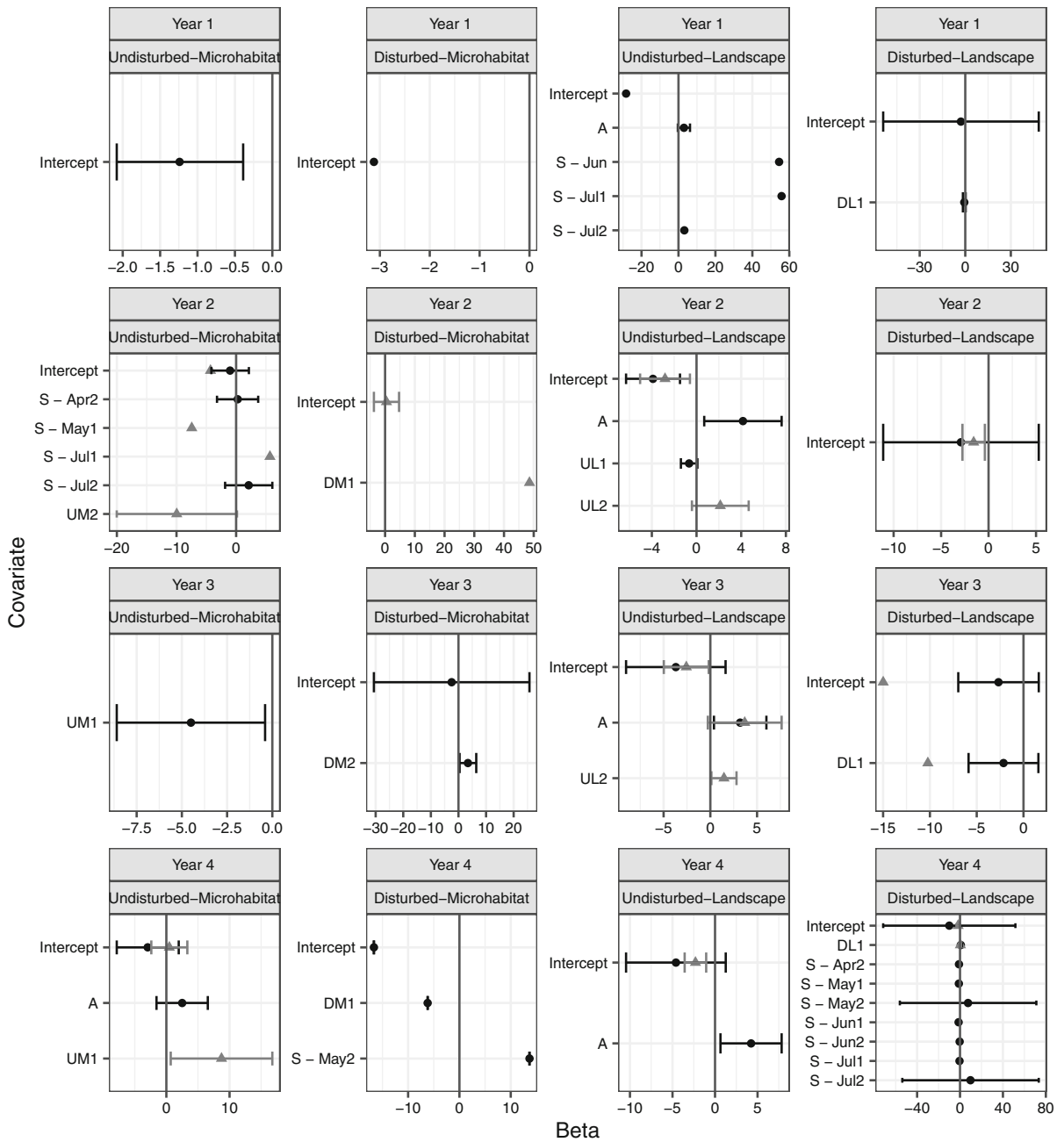


**Fig. 2** Model averaged beta values and 95% Confidence Intervals for probability of settlement ( $\gamma$ ; black circles) and vacancy ( $\epsilon$ ; gray triangles)

was constant ( $\gamma = 0.22 \pm 0.08$ ). Year 2 probability of settlement varied across trapping sessions (Fig. 10a in Online Appendix). Year 3 probability of settlement increased as mean slope increased and mean substrate compaction decreased (UM1; Fig. 10b in Online Appendix). Year 4 probability of settlement increased

as percent of occupied surrounding arrays increased (Fig. 10c in Online Appendix). On the disturbed array, year 1 probability of settlement was constant ( $\gamma = 0.09 \pm 0.04$ ) and year 2 was inestimable, most likely due to the sparsity of data on the disturbed array. Probability of settlement in year 3 increased as percent

**Table 2** Covariates from each of the top models for the microhabitat and landscape dynamic occupancy models from the undisturbed and disturbed arrays

|                          | Year | Use                       | Settlement                           | Vacancy                         |
|--------------------------|------|---------------------------|--------------------------------------|---------------------------------|
| Undisturbed-microhabitat | 1    | UM1 (↑slope, ↓compaction) | C                                    | NE                              |
|                          | 2    | UM2 (↑oak-litter)         | ↑↓S                                  | UM2 (↑oak-litter) + ↑S          |
|                          | 3    | UM2 (↑oak-litter)         | UM1 (↑slope, ↓compaction)            | NE                              |
|                          | 4    | UM1 (↑slope, ↓compaction) | ↑A                                   | UM1 (↓slope, ↑compaction)       |
| Undisturbed-landscape    | 1    | C                         | ↑A + ↑↓S                             | NE                              |
|                          | 2    | C                         | UL1 (↓large-clumpy sand) + ↑A        | UL2 (↑large-complex oak)        |
|                          | 3    | UL1 (↑large-clumpy sand)  | ↑A                                   | UL2 (↑large-complex oak) + ↑A   |
|                          | 4    | UL2 (↓large-complex oak)  | ↑A                                   | C                               |
| Disturbed-microhabitat   | 1    | DM2 (↑sand, ↓oak-litter)  | C                                    | NE                              |
|                          | 2    | DM1 (↑slope, ↓compaction) | NE                                   | DM1 (↓slope, ↑compaction)       |
|                          | 3    | C                         | DM2 (↑sand, ↓oak-litter)             | NE                              |
|                          | 4    | DM2 (↑sand, ↓oak-litter)  | DM1 (↑slope, ↓compaction) + ↑S       | NE                              |
| Disturbed-landscape      | 1    | C                         | DL1 (↑oak, ↓sand–road/well-pad)      | NE                              |
|                          | 2    | C                         | C                                    | C                               |
|                          | 3    | C                         | DL1 (↑oak, ↓sand–road/well-pad)      | DL1 (↓Oak, ↑Sand–road/well-pad) |
|                          | 4    | C                         | DL1 (↓Oak, ↑Sand–Road/Well-pad) + ↑S | DL1 (↓Oak, ↑Sand–road/well-pad) |

Model covariates are: *C* constant model; *A* autocovariate; *S* session (time effect); *NE* not estimable

cover of sand increased and percent covers of shinnery oak and litter decreased (DM2; Fig. 10d in Online Appendix). Finally, in year 4, probability of settlement increased as mean slope increased and mean substrate compaction decreased (DM1; Fig. 10e in Online Appendix); however, it was only estimable in the middle and final trapping sessions (again, probably due to sparsity of data during the other trapping sessions).

For microhabitat models, probability of vacancy was inestimable for years 1 and 3 on the undisturbed array and years 1, 3, and 4 on the disturbed array (Table 2). On the undisturbed array, in year 2, probability of vacancy decreased as percent cover of shinnery oak and litter decreased (UM2), but was only estimable early and mid-season (Fig. 11a in Online Appendix). In year 4, probability of vacancy increased as mean slope decreased and mean substrate compaction increased (UM1; Fig. 11b in Online

Appendix). On the disturbed array, in year 2, probability of vacancy increased as mean substrate compaction increased (DM1; Fig. 11c in Online Appendix).

For landscape models, settlement probabilities on the undisturbed array were consistently best predicted by models that included the spatial autocovariate (percent occupied surrounding sub-grids; Tables 1, 2). For all four years, probability of settlement increased as percent of occupied surrounding arrays increased (Fig. 12a–c in Online Appendix). Probability of settlement in year 1 also had an additive effect of session, limiting estimates to June–July and July–July transition periods. In year 2, probability of settlement also decreased as area and clumpiness of sand patches increased (UL1; Fig. 12b in Online Appendix). On the disturbed array for years 1 and 3, probability of settlement decreased as patch areas of sand and road/well-pad increased (DL1; Fig. 12d in Online

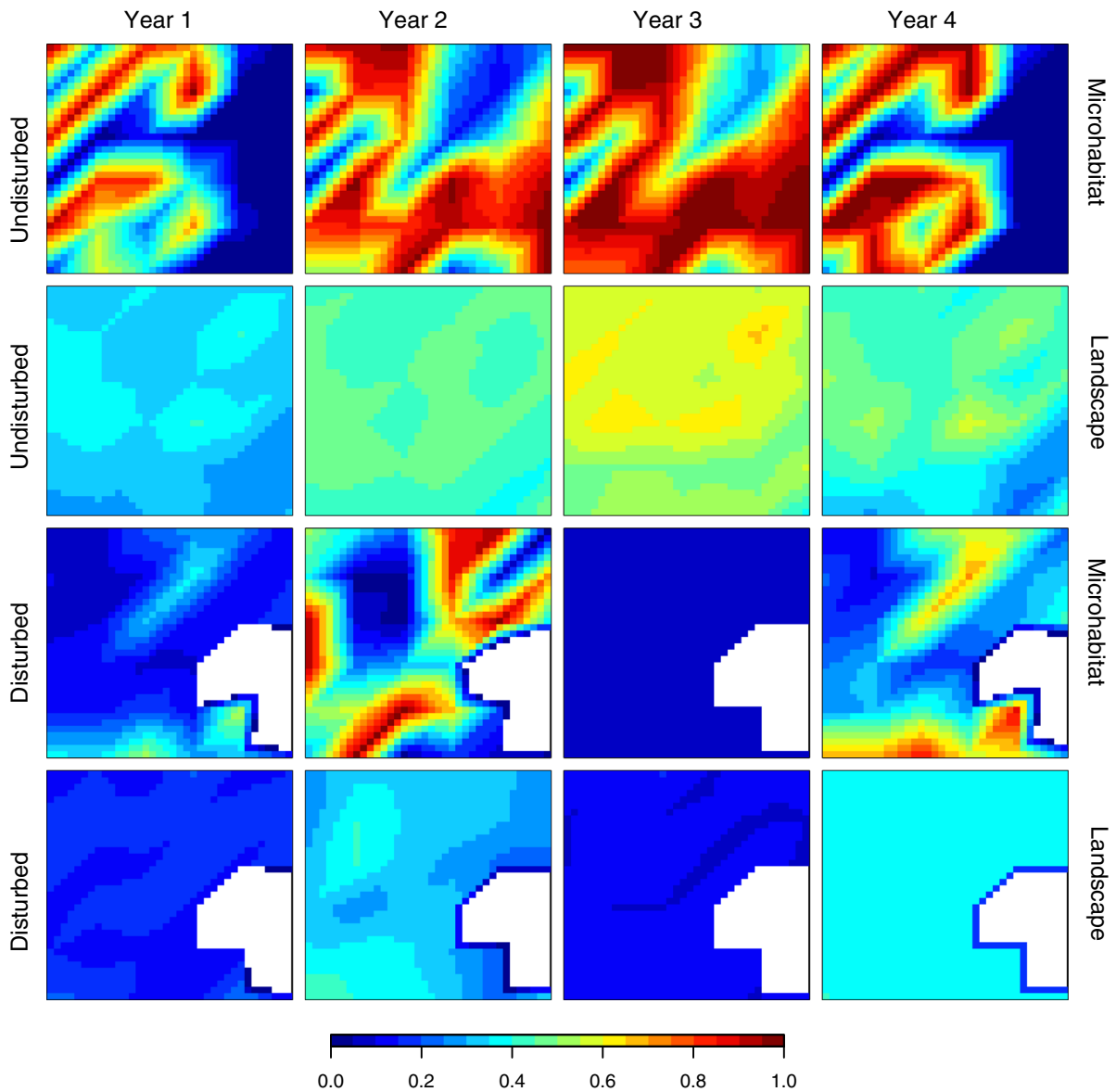


**Fig. 3** Predicted probability of use ( $\psi$ ) by array, year, and scale. The  $\psi$  values for each panel are the model averaged results for each model, using the covariates from Fig. 1 above. Values have been linearly interpolated across the site.

Undisturbed landscapes cover N 32.1291–32.1322° and W 102.6782–102.6745°, and disturbed landscapes cover N 32.1293–32.1324° and W 102.7416–102.7379°

Appendix), but in year 4, probability of settlement increased as patch areas of sand and road/well-pad increased (DL1; Fig. 12e in Online Appendix). In year 4, we also saw an additive effect of session: early June and early August were the only sessions in which probability of settlement was estimable (Fig. 12e in

Online Appendix). Finally, for year 2, probability of settlement was constant ( $\gamma = 0.16 \pm 0.07$ ).

For landscape models at both arrays, probability of vacancy was inestimable for year 1 (Table 2). On the undisturbed array, in years 2 and 3, probability of vacancy increased as area and fractal dimension of shinnery oak patches increased (UL2; Fig. 13a, b in

Online Appendix). Finally, in year 4, probability of vacancy was constant ( $\varepsilon = 0.09 \pm 0.03$ ). On the disturbed array, in year 2, probability of vacancy was constant ( $\varepsilon = 0.06 \pm 0.02$ ), while for years 3 and 4, probability of vacancy increased as patch areas of sand and road/well-pad increased (DL1; Fig. 13c in Online Appendix).

For landscape models, we saw variation in net differences between probability of settlement and probability of vacancy in years 2 through 4 (when both parameters are estimable; Fig. 4). On the undisturbed array, probability of settlement was equal to or higher than probability of vacancy in year 2 (Fig. 4). This changed in years 3 and 4; in year 3 probability of settlement was equal to or lower than probability of vacancy, a trend that strengthened in year 4 (Fig. 4). On the disturbed array, again we saw few consistent patterns in net differences between probability of settlement and probability of vacancy in years 2 through 4 (when both parameters are estimable; Table 1). In years 2 and 4, probabilities of settlement and vacancy were constant resulting in a consistently high probability of settlement across the array (Fig. 4). In year 3, there was a split where some areas had fairly high probabilities of settlement, while others had high probabilities of vacancy (Fig. 4). In both years 3 and 4, probability of vacancy increased as patch areas of sand and road/well-pad increased (DL1), but because probability of settlement for these 2 years had opposite relationships to patch areas of sand and road/well-pad, we saw different patterns in probabilities of settlement and vacancy across the array (Fig. 4).

## Discussion

The overarching pattern in our study was that use, settlement, and vacancy in *S. arenicolus* populations are dynamic within its habitat at multiple scales, and no single variable or scale can consistently predict those dynamics over time. A general trend in our results was that microhabitat variables predicted the probability of use for *S. arenicolus* better than the constant model across both arrays, whereas landscape variables generally failed to predict use better than the constant model, especially for the disturbed array (Table 2). With respect to settlement and vacancy, we observed an opposite, albeit weaker, trend for the disturbed array. Microhabitat variables failed to

predict settlement and vacancy better than the constant model or were not estimable at the disturbed array, whereas landscape variables generally predicted settlement and, to a lesser extent, vacancy better than the constant model. Microhabitat and landscape variables generally predicted settlement and vacancy at the undisturbed array better than the constant model across most years (Table 2).

These observations suggest the habitat features we measured influence different population processes at different spatial scales (Wiens et al. 1993). For example, at the microhabitat scale, use is important because it determines day-to-day behaviors related to individual survival: food availability, thermoregulation sites, and shelter from predators (Wiens et al. 1993). In the larger landscape context, settlement and vacancy are important because they reflect larger scale population activities such as (1) mate searching and nest-site selection (Hill and Fitzgerald 2007 unpublished report), (2) dispersal of juvenile *S. arenicolus* from natal areas (Ryberg et al. 2013), or (3) movements between sub-populations (Blevins and With 2011). Below, we discuss in greater detail the observed spatiotemporal patterns of use, settlement, and vacancy by *S. arenicolus* and their relationship to specific landscape features at different scales.

## Use

Previous studies have identified that within the dune ecosystem, *S. arenicolus* consistently favors specific microhabitat variables reflecting the importance of large deep dune blowouts (Fitzgerald et al. 1997; Fitzgerald and Painter 2009; Hibbitts et al. 2013). Our results support previous findings, as steep slopes, loose sand, and shinnery oak cover were good predictors of fine-scale variation in probability of use at the microhabitat scale (i.e., predicted use better than the constant model). Hibbitts et al. (2013) also showed *S. arenicolus* preferred steeper, sandy slopes and less compact soils at the microhabitat scale in fragmented and unfragmented areas. On our disturbed array, *S. arenicolus* also used areas with steeper, less compact, sandy slopes and less shinnery oak cover, although the best predictors of use varied over space and time (discussed below).

We observed complex temporal dynamics in habitat use that have conservation implications for this species, as well as other habitat specialists. Habitat use

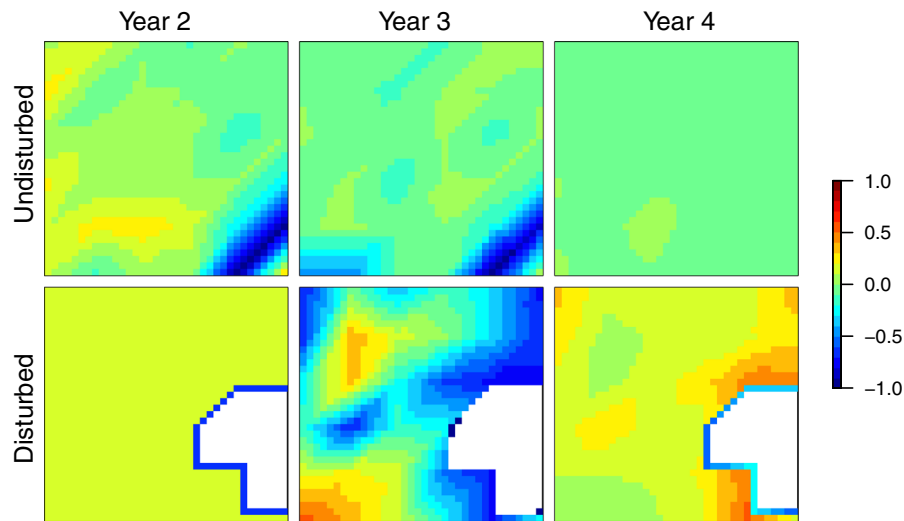


**Fig. 4** The difference between predicted probability of settlement ( $\gamma$ ) and predicted probability of vacancy ( $\epsilon$ ) from the model averaged values from the top models from the landscape analyses, for each sub-grid. If settlement was greater than vacancy, values were positive; if settlement was less than vacancy, values were negative. Probability of vacancy was

inestimable for year 1 at both arrays, so those estimates were not included. Values have been linearly interpolated across the site. Undisturbed landscapes cover N 32.1291–32.1322° and W 102.6782–102.6745°, and disturbed landscapes cover N 32.1293–32.1324° and W 102.7416–102.7379°

associations can change over time, expanding in optimal resource years and becoming more restrictive in suboptimal resource years (Sergio and Newton 2003; Hurme et al. 2008). Sergio et al. (2003) found that *Milvus migrans* (black kite) occupied more low-quality territories when population densities were higher, while high quality territories were preferred in all years. Additionally, Hurme et al. (2008) showed *Pteromys volans* (Siberian flying squirrels) constantly occupied some habitat patches, while also showing intermittent occupancy of patches of lesser quality that may have been important for maintaining networks of habitat. The observed spatio-temporal patterns of use by *S. arenicolus* on the undisturbed array are consistent with these studies and likely also reflect expansion during optimal resource years to include use of lower quality habitat that is more dominated by shinnery oak, and contraction during sub-optimal resource years to areas of higher quality habitat with steep, sandy slopes preferred by the species (Fitzgerald and Painter 2009; Hibbitts et al. 2013; Ryberg et al. 2013, 2015). Recognizing these temporal patterns of expanding and contracting habitat use has important implications for conservation. For *S. arenicolus*, it has been shown that integrity of populations at large scales

depends on diffusion dispersal and neighborhood dynamics (Ryberg et al. 2013; Walkup et al. 2017). Thus, it is critical to the persistence of this species, and probably many others, that portions of habitat that are used intermittently be preserved to ensure connectivity of habitat patches.

The best predictors of use at the disturbed array varied unpredictably over space and time as compared to the undisturbed array. Hibbitts et al. (2017) and Young et al. (2018) showed that even the smallest road tracks in the region can act as a barrier for *S. arenicolus*, which may partially explain why there were two core areas of habitat used on the disturbed array to the north and south of the road. Populations of *S. arenicolus* in even moderately fragmented habitats are typically smaller and more isolated, and exhibit dramatic disruption in demographic structure that frequently leads to local extirpations (Smolensky and Fitzgerald 2011; Leavitt and Fitzgerald 2013; Walkup et al. 2017). The spatiotemporal unpredictability observed in habitat use at the disturbed array in this study is consistent with expectations for a fragmented population of *S. arenicolus*.

## Settlement and vacancy

Landscape features predicted the probability of settlement and vacancy parameters better than the microhabitat variables for both the undisturbed and disturbed arrays. The only models for which the autocovariate was consistently and highly predictive were for probability of settlement in the undisturbed array at the landscape scale. In other words, simply the presence of *S. arenicolus* in some areas at the undisturbed array was the best predictor of settlement dynamics. This spatiotemporal pattern of settlement suggests that some areas act as sources for *S. arenicolus*, contributing enough individuals to potentially mask any other effects of the landscape on the population. Networks of *S. arenicolus* neighborhoods in uninterrupted habitats have already been shown to exhibit population dynamics (i.e., survival and recruitment dynamics) linked to landscape configuration that are consistent with source-sink metapopulation structures (Ryberg et al. 2013), and results from this study support those conclusions. However, the autocovariate generally did not influence use, settlement, or vacancy on the disturbed array, which suggests that the *S. arenicolus* population on the disturbed array was not functioning like other populations in less disturbed habitat. Instead, the population on the disturbed array appeared to use two areas of habitat that shifted and sometimes disappeared over time, without any expansion across the landscape dependent on the surrounding lizard density, as would be expected in typical source-sink dynamics (Eriksson 1996; Diffendorfer 1998). As the prevalence of such disturbances grows in the region, these results predict an erosion of the neighborhood connectivity necessary to maintain *S. arenicolus* dispersal and source-sink dynamics. This could lead to local extinctions (Leavitt and Fitzgerald 2013; Walkup et al. 2017) and create disjunct, conservation-reliant, populations of the species in the future (i.e., requiring assisted migration or supplementation for persistence).

The best predictor of future settlement is the present location of *S. arenicolus*. This is supported by the importance of the autocovariate in determining settlement dynamics in undisturbed habitat. This observation helps frame the scale of spatiotemporal dynamics of settlement and vacancy in undisturbed habitats to within the breeding season and between years. This is in contrast to studies of regional or range-wide patch

occupancy dynamics, which occur over much larger spatiotemporal scales in this species (Walkup et al. 2018). For example, during the breeding season, settlement increased earlier in the active season when mating occurs and late in the season when hatchlings emerge (Tables 9, 12 in Online Appendix; Fitzgerald and Painter 2009). Settlement was lowest in early spring and during the hottest part of the activity season (Table 12 in Online Appendix). These fine-scale spatiotemporal dynamics highlight the importance of individual movements of *S. arenicolus*, including both lifetime and within-season movements (Young et al. 2018), in determining patterns of use, settlement, and vacancy in undisturbed habitats. Moreover, any interference of fine-scale spatiotemporal dynamics from known barriers to *S. arenicolus* movements (e.g., caliche roads and well-pads; Hibbitts et al. 2017; Young et al. 2018) act to disrupt patterns of use, settlement, and vacancy in disturbed habitats. The observed decrease in settlement and increase in vacancy probabilities in the presence of roads and well-pads at the disturbed array supports this idea (Table 2). Indeed, the small road bisecting the disturbed array in our study probably acted as a barrier to individual lizard movements, providing a plausible explanation for the observed spatiotemporal unpredictability in use, settlement, and vacancy at that site.

In summary, our study illustrates how some undisturbed *S. arenicolus* habitats in this ecosystem may be used constantly, while others may be used intermittently, but repeatedly, over time. As fragmentation of contiguous habitat spreads throughout this ecosystem (EIA 2017; Fitzgerald et al. 2018; Pierre et al. 2018; Wolaver et al. 2018a, b), intermittent habitat use by *S. arenicolus* could become proportionally more common through the reduction of constantly used habitat, which if improperly interpreted, could be mis-used to justify more development in these presumably unoccupied habitat patches. This in turn could lead to an erosion of habitat continuity, disjunct populations, and even more intermittently occupied habitat patches. These findings carry three important and interrelated conservation implications for *S. arenicolus* and other habitat specialists. First, even though a habitat specialist may appear to occupy a large area, narrow resource dependence of the species may allow only a small fraction of that area to be used constantly (e.g., Jetz et al. 2008). The loss of these small, critically

important, areas can have profound effects on the local population and negate potential benefits of conservation actions elsewhere (Runge et al. 2014). For *S. arenicolus*, it was shown that populations in areas of high quality habitat that are constantly used produce the surplus of hatchlings that diffuse across continuous habitat. These sources are critical to the persistence of the species across broader expanses of habitat of varying quality (Ryberg et al. 2013; Walkup et al. 2017). Second, integrating temporal dynamics of intermittently used areas into conservation planning for habitat specialists may be challenging, but critical for protecting key locations that support source-sink dynamics (Runge et al. 2014). The first two conservation implications frame the final: spatially-discrete but temporally-linked areas should be conserved at a scale that provides the greatest chance for persistence of populations over the long term in the face of variable environmental conditions.

**Acknowledgements** Big thanks to all our field technicians, without whom this work would not have happened: Connor Adams, Jonathon Bolton, Sarah Bord, Logan Ediger, Aubany Fields, Shelby Frizzell, Aleyda Galan, Ana Hernandez, Cameron Hodges, Daniel Lay, Timmy Songer, Brooke Tolson, Scott Wahlberg, and J.M. Weidler. Thanks to Megan Young for assistance and logistics in the field. This is publication number 1620 of the Biodiversity Research and Teaching Collections at Texas A&M University.

**Funding** This study was funded by the Texas Comptroller of Public Accounts and the Texas A&M University's College of Agriculture and Life Sciences Tom Slick Graduate Fellowship.

#### Compliance with ethical standards

**Conflict of interest** All authors that they have no conflict of interest.

#### References

- Addicott JF, Aho JM, Antolin MF, Padilla DK, Richardson JS, Soluk DA (1987) Ecological neighborhoods: scaling environmental patterns. *Oikos* 49:340–346
- Augustin NH, Muggleston MA, Buckland ST (1996) An autologistic model for the spatial distribution of wildlife. *J Appl Ecol* 33:339–347
- Betts MG, Diamond AW, Forbes GJ, Villiard M-A, Gunn JS (2006) The importance of spatial autocorrelation, extent and resolution in predicting forest bird occurrence. *Ecol Model* 191:197–224
- Betts MG, Rodenhouse NL, Sillett TS, Doran PJ, Holmes RT (2008) Dynamic occupancy models reveal within-breeding season movement up a habitat quality gradient by a migratory songbird. *Ecography* 31:592–600
- Blevins E, With KA (2011) Landscape context matters: local habitat and landscape effects on the abundance and patch occupancy of collared lizards in managed grasslands. *Landscape Ecol* 26:37–850
- Buckland ST, Burnham KP, Augustin NH (1997) Model selection: an integral part of inference. *Biometrics* 53:603–618
- Burnham KP, Anderson DR (2002) Model selection and multimodel inference: a practical information-theoretic approach, 2nd edn. Springer, New York
- Chammem M, Selmi S, Khorchani T, Nouira S (2012) Using a capture-recapture approach for modelling the detectability and distribution of Houbra Bustard in southern Tunisia. *Bird Conserv Int* 22:288–298
- Cornell KL, Donovan TM (2010) Scale-dependent mechanisms of habitat selection for a migratory passerine: an experimental approach. *Auk* 127:899–908
- Diffendorfer JE (1998) Testing models of source-sink dynamics and balanced dispersal. *Oikos* 81:417–433
- Efford MG, Dawson DK (2012) Occupancy in continuous habitat. *Ecosphere* 34:32
- EIA. 2017. Rankings: crude oil production, November 2016 (thousand barrels). U.S. Energy Information Administration (EIA). <http://www.eia.gov/state/rankings/?sid=TX#series/46>. Accessed 25 Feb 2017
- Eriksson O (1996) Regional dynamics of plants: a review of evidence for remnant, source-sink and metapopulations. *Oikos* 77:248–258
- Fiske I, Chandler R (2011) Unmarked: an R package for fitting hierarchical models of wildlife occurrence and abundance. *J Stat Softw* 43:1–23
- Fitzgerald LA (2012) Finding and capturing reptiles. In: McDiarmid RW, Foster MS, Guyer C, Gibbons JW, Chernoff N (eds) Measuring and monitoring biological diversity: standard methods for reptiles. University of California Press, Berkeley, pp 77–88
- Fitzgerald LA, Painter CW (2009) Dunes sagebrush lizard. In: Jones L, Lovich R (eds) Lizards of the American Southwest. Rio Nuevo, Tucson, pp 198–201
- Fitzgerald LA, Painter CW, Sias DW, Snell HW (1997) The range, distribution and habitat of *Sceloporus arenicolus* in New Mexico. Final Report, New Mexico Department of Game and Fish, Santa Fe, New Mexico, USA
- Fitzgerald LA, Walkup D, Chyn K, Buchholtz E, Angeli N, Parker M (2018) The future for reptiles: advances and challenges in the Anthropocene. In: DellaSala D, Goldstein M (eds) Encyclopedia of the Anthropocene. Elsevier, Oxford, pp 163–174
- Frey SJK, Strong AM, McFarland KP (2012) The relative contribution of local habitat and landscape context to metapopulation processes: a dynamic occupancy modeling approach. *Ecography* 35:581–589
- Galley JE (1958) Oil and geology in the permian basin of Texas and New Mexico: North America. Habitat of Oil, AAPG special volume, pp 395–446

- González-Megías A, Gómez JM, Sánchez-Piñero F (2005) Regional dynamics of a patchily distributed herbivore along an altitudinal gradient. *Ecol Entomol* 30:706–713
- Gotelli NJ, Ellison AM (2004) A primer of ecological statistics. Sinauer Associates Inc., Sunderland
- Haggerty J, Gude PH, Delorey M, Rasker R (2014) Long-term effects of income specialization in oil and gas extraction: the U.S. West, 1980–2011. *Energ Econ* 45:186–195
- Hammer Ø, Harper DAT, Ryan PD (2001) PAST: paleontological statistics software package for education and data analysis. *Palaeontol Electron* 4:1–9
- Herse MR, Estey ME, Moore PJ, Sandercock BK, Boyle WA (2017) Landscape context drive breeding habitat selection by an enigmatic grassland songbird. *Landscape Ecol* 32:2351–2364
- Hibbitts TJ, Ryberg WA, Adams CS, Fields AM, Lay D, Young ME (2013) Microhabitat selection by a habitat specialist and generalist in both fragmented and unfragmented landscapes. *Herpetol Conserv Bio* 8:104–113
- Hibbitts TJ, Fitzgerald LA, Walkup DK, Ryberg WA (2017) Why didn't the lizard cross the road? Dunes sagebrush lizards exhibit road-avoidance behavior. *Wildlife Res* 44:194–199
- Hurme E, Mönkkönen M, Reunanen P, Nikula A, Nivala V (2008) Temporal patch occupancy dynamics of the Siberian flying squirrel in a boreal forest landscape. *Ecography* 31:469–476
- Jetz W, Sekercioglu CH, Watson JEM (2008) Ecological correlates and conservation implications of overestimating species geographic ranges. *Conserv Biol* 22:110–119
- Krohne DT, Burgin AB (1990) The scale of demographic heterogeneity in a population of *Peromyscus leucopus*. *Oecologia* 82:97–101
- Laurencio LR, Fitzgerald LA (2010) Atlas of distribution and habitat of the dunes sagebrush lizard (*Sceloporus arenicolus*) in New Mexico. Texas Cooperative Wildlife Collection, Department of Wildlife and Fisheries Sciences, Texas A&M University, College Station. ISBN# 978-0-615-40937-5
- Leavitt DJ, Fitzgerald LA (2013) Disassembly of a dune-dwelling lizard community due to landscape fragmentation. *Ecosphere* 4:97
- Levin SA (1992) The problem of pattern and scale in ecology: the Robert H. MacArthur award lecture. *Ecology* 73:1943–1967
- MacKenzie DI, Nichols JD, Hines JE, Knutson MG, Franklin AB (2003) Estimating site occupancy, colonization, and local extinction when a species is detected imperfectly. *Ecology* 84:2200–2207
- Mazerolle MJ (2016) AICcmodavg: model selection and multimodel inferences based on (Q)AIC(c). R package version 2.1-0. <https://cran.r-project.org/package=AICcmodavg>
- McClure CJW, Hill GE (2012) Dynamic versus static occupancy: how stable are habitat associations through a breeding season? *Ecosphere* 3(7):60
- McClure CJW, Rolek BW, Hill GE (2012) Predicting occupancy of wintering migratory birds: is microhabitat information necessary? *Condor* 114:482–490
- McGarigal K, Cushman SA, Ene E (2012) FRAGSTATS v4: spatial pattern analysis program for categorical and continuous maps. Computer software program produced by the authors at the University of Massachusetts, Amherst. <http://www.umass.edu/landeco/research/fragstats/fragstats.html>
- Merriam G (1995) Movement in spatially divided populations: responses to landscape structure. In: Lidicker WZ Jr (ed) Landscape approaches in mammalian ecology and conservation. University of Minnesota Press, Minneapolis, pp 64–77
- Michael DR, Ikin K, Crane M, Okada S, Lindenmayer DB (2017) Scale-dependent occupancy patterns in reptiles across topographically different landscapes. *Ecography* 40:415–424
- Pierre JP, Wolaver BD, Labay BJ, LaDuc TJ, Duran CM, Ryberg WA, Hibbitts TJ, Andrews JR (2018) Comparison of recent oil and gas, wind energy, and other anthropogenic landscape alteration factors in Texas through 2014. *Environ Manage* 61:805–818
- R Core Team (2018) R: a language and environment for statistical computing. R Foundation for Statistical Computing, Vienna
- Runge CA, Martin TG, Possingham HP, Willis SG, Fuller RA (2014) Conserving mobile species. *Front Ecol Environ* 12:395–402
- Ryberg WA, Fitzgerald LA (2015) Sand grain size composition influences subsurface oxygen diffusion and distribution of an endemic, psammophilic lizard. *J Zool* 295:116–121
- Ryberg WA, Fitzgerald LA (2016) Landscape composition, not connectivity, determines metacommunity structure across multiple scales. *Ecography* 39:932–941
- Ryberg WA, Hill MT, Lay D, Fitzgerald LA (2012) Observations on the nesting ecology and early life history of the Dunes Sagebrush Lizard (*Sceloporus arenicolus*). *West N Am Nat* 72:582–586
- Ryberg WA, Hill MT, Painter CW, Fitzgerald LA (2013) Landscape pattern determines neighborhood size and structure within a lizard population. *PLoS ONE* 8:e56856
- Ryberg WA, Hill MT, Painter CW, Fitzgerald LA (2015) Linking irreplaceable landforms in a self-organizing landscape to sensitivity of population vital rates for an ecological specialist. *Conserv Biol* 29:888–898
- Sergio F, Newton I (2003) Occupancy as a measure of territory quality. *J Anim Ecol* 72:857–865
- Shaver GR (2005) Spatial heterogeneity: past, present, and future. In: Lovett GM, Turner MG, Jones CG, Weathers KC (eds) Ecosystem function in heterogeneous landscapes. Springer, New York, pp 443–449
- Smolensky NL, Fitzgerald LF (2011) Population variation in dune-dwelling lizards in response to patch size, patch quality, and oil and gas development. *Southwest Nat* 56:315–324
- Sozio G, Mortelliti A, Boccacci F, Ranchelli E, Battisti C, Boitani L (2013) Conservation of species occupying ephemeral and patchy habitats in agricultural landscapes: the case of the Eurasian reed warbler. *Landscape Urban Plan* 119:9–19
- Turner MG (1990) Spatial and temporal analysis of landscape patterns. *Landscape Ecol* 4:21–30
- Turner MG, Chapin FS (2005) Causes and consequences of spatial heterogeneity in ecosystem function. In: Lovett GM, Turner MG, Jones CG, Weathers KC (eds) Ecosystem function in heterogeneous landscapes. Springer, New York, pp 9–30



- Walkup DK, Leavitt DJ, Fitzgerald LA (2017) Effects of habitat fragmentation on population structure of dune-dwelling lizards. *Ecosphere* 8:e01729
- Walkup DK, Ryberg WA, Fitzgerald LA, Hibbitts TJ (2018) Occupancy and detection of an endemic habitat specialist, the dunes sagebrush lizard (*Sceloporus arenicolus*). *Herpetol Conserv Biol* 13(3):497–506
- Webb MH, Terauds A, Tulloch A, Bell P, Stojanovic D, Heinsohn R (2017) The importance of incorporating functional habitats into conservation planning for highly mobile species in dynamic systems. *Conserv Biol* 31:1018–1028
- Wiens JA, Stenseth NC, Van Horne B, Ims RA (1993) Ecological mechanisms and landscape ecology. *Oikos* 66:369–380
- Wolaver BD, Pierre JP, Ikonnikova SA, Andrews JR, McDaid G, Ryberg WA, Hibbitts TJ, Duran CM, Labay BJ, LaDuc TJ (2018a) An improved approach for forecasting ecological impacts from future drilling in unconventional shale oil and gas plays. *Environ Manage* 62:323–333
- Wolaver BD, Pierre JP, Labay BJ, LaDuc TJ, Duran CM, Ryberg WA, Hibbitts TJ (2018b) An approach for evaluating changes in land-use from energy sprawl and other anthropogenic activities with implications for biotic resource management. *Environ Earth Sci* 77:171
- Ye X, Wang T, Skidmore AK (2013a) Spatial pattern of habitat quality modulates population persistence in fragmented landscapes. *Ecol Res* 28:949–958
- Ye X, Skidmore AK, Wang T (2013b) Within-patch habitat quality determines the resilience of specialist species in fragmented landscapes. *Landscape Ecol* 28:135–147
- Young ME, Ryberg WA, Fitzgerald LA, Hibbitts TJ (2018) Fragmentation alters home range and movements of the dunes sagebrush lizard (*Sceloporus arenicolus*). *Can J Zool* 96:905–912

**Publisher's Note** Springer Nature remains neutral with regard to jurisdictional claims in published maps and institutional affiliations.